HOKKAIDO UNIVERSITY

Title	Latent heat storage capacity of NiTi shape memory alloy
Author(s)	Kato, Hiroyuki
Citation	Journal of materials science, 56(13), 8243-8250 https://doi.org/10.1007/s10853-021-05777-6
Issue Date	2021-01-19
Doc URL	http://hdl.handle.net/2115/83841
Rights	This is a post-peer-review, pre-copyedit version of an article published in Journal of Materials Science. The final authenticated version is available online at: http://dx.doi.org/10.1007/s10853-021-05777-6
Type	article (author version)
File Information	baigaesi_11.pdf

Instructions for use

Hokkaido University Collection of Scholarly and Academic Papers : HUSCAP

Author: Kato, Hiroyuki;
Title: Latent heat storage capacity of NiTi shape memory alloy
Journal: Journal of materials science
Publisher: Springer
Year 2021
Volume 56(13) 8243-8250
ISSN: 0022-2461
DOI 10.1007/s10853-021-05777-6

Latent heat storage capacity of NiTi shape memory alloy

Hiroyuki Kato

Mechanical and Space Engineering, Hokkaido University, Sapporo 060-8628, Japan

ABSTRACT

The largest amount of latent heat of the martensitic transformation in Nickel Titanium shape memory alloy was explored. The measured amounts of heat in the alloys with different compositions between 48.0 at.% Ni and 51.0 at.% Ni were compared. The largest amounts of −37.8 J/g in absorption and 34.8 J/g in emission were obtained as the averaged values of several samples with equiatomic composition. These magnitudes are close to those of novel heat-storage ceramics, VO_2 (51 J/g) and Ti_3O_5 (60 J/g), suggesting the NiTi alloy is potential candidate for heat storage material.

Keywords Shape Memory Alloy; NiTi; Latent heat; Heat storage; Phase Change Material

Introduction

The solid-state heat pumping [1] is one of the primary objectives of the recent research on phase change materials (PCMs). The switching of heat flow by means of external potential field is termed “active caloric effect”. Among various PCMs in solids, shape memory alloy (SMA), which makes use of the latent heat associated with the stress-induced martensitic transformation, is a promising candidate for elasto-caloric material [2-5].

As for passive caloric effect, the latent heat storage of PCM has also been relevant to heat-transfer engineering [6]. The feasibility of SMA for heat storage was studied in this paper. A

candidate for heat storage PCM is expected to show large amount of latent heat. Previous results listed in Table 1 indicates that the amount of heat of Nickel Titanium (NiTi) alloy was larger than those of the other SMAs [7-17]. It is known that the alloy undergoes the thermoelastic transformation from the B2 ordered beta phase to the B19' martensite [18].

A considerable amount of works on the latent heat of the martensitic transformation have been reported since the beginning of the study on NiTi [19]. The largest value in Table 1 was 35 J/g [15], modest values were 30.8 J/g [16] and 31.7 J/g [20], and rather small values of 20 J/g were reported [21, 22]. Present author confirmed the latent heat of 23.6 J/g of a work-hardened and age-hardened $Ti_{49.5}Ni_{50.5}$ alloy satisfied the Clausius-Clapeyron relation [23]. It is reasonable to consider that the value may be different depending on the state of sample. Present study explored the upper limit value in order to specify the range.

The largest value is of interest not only because of potential engineering application of heat storage PCM but also because of the need for material constant inherent to crystal lattice, of which value is appreciated in thermodynamics. If a material includes some lattice defects, the latent heat would be smaller than that of the perfect crystal. The heat value of lattice shall be used or calculated in, *e.g* , phase field method, CALPHAD, and molecular dynamics.

In this study, the largest amount of latent heat was explored by considering;

(i) The homogeneous beta-phase free from plastic work and precipitate of second phases. Mechanical property [23,28] does not matter.

(ii) The stability of the beta phase of Ti-rich alloy is limited in narrow composition range of the phase diagram [24-25], as seen in Fig. 1.

(iii) The hysteresis in the transformation temperatures, Ms-Mf or Af-As, is the measure of the homogeneity of composition. The Ms and Mf is the temperatures at which the martensitic transformation starts and finishes, respectively. The As and Af are those for the reverse transformation. It was reported that the hysteresis became wide when the second phase precipitated [26-32].

(iv) The heat resistance between the sample and stage is the major origin of the heat loss in DSC measurement [33,34].

Materials and methods

Commercial products of NiTi shape memory alloys were supplied by Furukawa techno material Co. LTD. As-received samples were cold-drawn wires of Ti-48.0, 48.5, 49.0, 49.5, 50.0, 50.5, 50.6 at.% Ni and hot-rolled plates of Ti-49.5, 50.0, 50.5 at.% Ni. These products include carbon not more than 300 ppm [35]. All samples were solution treated under the following processing;

1) Oxidation layers on the surface of as received wires and plates were removed by the aqueous solution of hydrofluoric acid and nitric acid.
2) The samples were sealed in the evacuated quartz tubes with titanium getters.
3) The encapsulated samples were annealed at 1,100 ℃ for 10 h. At this temperature, the alloys with Ni content larger than 49.5 at.% is in the homogeneity range, as seen in Fig. 1. In this figure, the samples used at present study are plotted by open circles.
4) Rapid quenching into ice water was done to obtain the beta phase at room temperature.

Table 1 Former data on the latent heat per unit weight of various shape memory alloys.

alloy	J/g	ref.	alloy	J/g	ref.
Cu-Zn-Al	2.3	[4]	Ni-Al-Mn-Fe	12.3	[11]
Cu-Al-Ni-Cr	7.4	[7]	Ni-30Mn-20Ga	6.3	[12]
Cu-Al-Ni	9.2	[8]	Ni-20Mn-25Ga	10.2	[13]
Fe-30Mn-6Si*	6.3	[9]	Co-Ni-Ga	1.3	[14]
Ni-36Al	5.9	[10]	Ni-Ti	~35	[15-18]

* in mass %

This study used a Shimadzu DSC-60 with the heating/cooling rate of 10 ℃/min. The values of temperature and heat flow were calibrated by the melting/solidifying temperature (156.6 ℃) and the latent heat (28.45 J/g) of a 4N purity Indium. The uncertainty in the measured latent heat was in the range of ±2 J/g for NiTi samples, as indicated by error bars, while the range was limited within ±0.5 J/g for pure Indium samples.

In principle, DSC measures the heat flow $\dot{Q}$ [W/g] of a sample at the heating/cooling rate of α [K/s] as a function of time t [s]. The latent heat per gram is given as

$$Q = \int \dot{Q}\,(t)\,dt = \frac{1}{\alpha}\int \dot{Q}\,(T)dT \quad , \qquad (1)$$

where $\int \dot{Q}\,(T)\,dT$ is the area of peak in DSC curve of unit mass. This relation indicates that the peak area changes in proportion to the rate α.

As a rate-independent physical property, the electrical resistance (ER) was measured by the four-point method with the direct current of 0.1 A. The ER was measured quasi-statically in slow heating/cooling rate less than 1 ℃/min, so that the result would not be affected by the inertia effect of heat transfer [33,34].

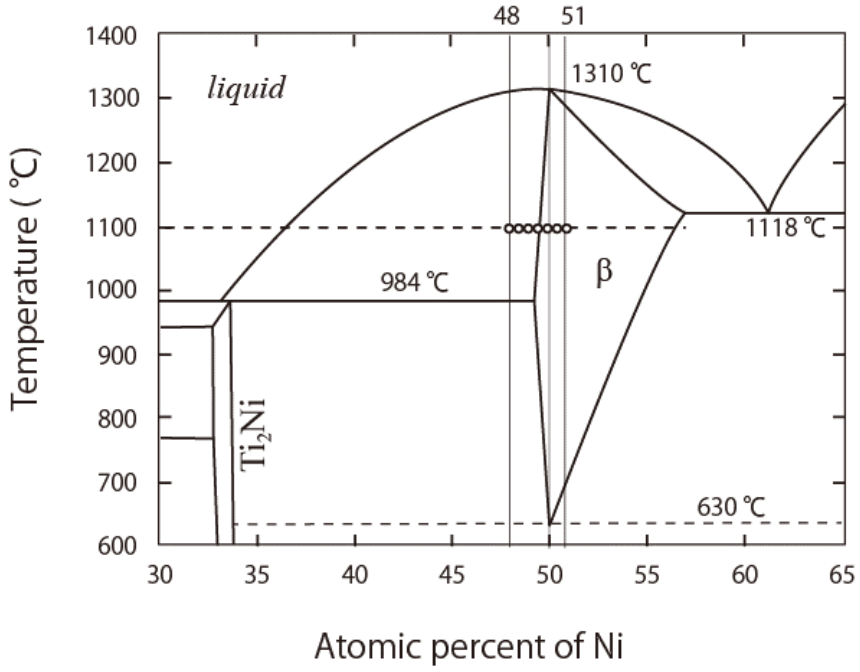

Fig. 1 The equilibrium phase diagram of NiTi alloy after Murray [25]. The compositions of the samples used at the present study are plotted by open circles.

Results

It is known that the amount of latent heat in NiTi alloy is different depending on the composition. A few systematic studies on the composition dependence have revealed that the maximum in the alloy presented at around the equiatomic composition [15,16]. Present study was concerned with the maximum value, so that the latent heat of the alloys with composition around 50.0 at.% Ni was examined.

First, the hysteresis of martensitic transformation of the samples used at present study was examined. The results of ER and DSC of the solution-treated wires of Ti- 49.5, 50.0, and 50.5 at.% Ni are shown in Fig. 2. The single inflection in ER curve and the single peak in DSC curve were due to the transformation of the B19' martensite [19, 26-32]. The ER and DSC curves showed almost identical Ms and As temperatures with each other.

The transformation temperatures, Ms, Mf, As, Af, were located at the inflection points in the ER curves; these are listed in Table 2. The inflection occurred in the temperature range between the Ms and Mf, and the As and Af. The present results show quite narrow hysteresis as compared with those in the ranges from 20 ℃ to 30 ℃ in Ref. [16,26,27,29-32]. The result indicates that the solution treated samples used at present study were homogeneous in composition, as mentioned above.

Table 2 The transformation temperatures (°C) determined by ER measurement

alloy	Ms	Mf	Ms−Mf	As	Af	Af−As
Ti-49.5 at. %Ni	66.0	53.8	12.2	83.0	95.7	12.7
Ti-50.0 at. %Ni	53.5	42.3	11.2	63.2	74.8	11.6
Ti-50.5 at. %Ni	7.5	- 3.9	11.4	26.6	38.3	11.7

The DSC results on the transformation temperature and the amount of latent heat are shown in Fig. 3. The upper and lower figure is the peak temperature of the cusp point in DSC peak during the reverse transformation and the corresponding amount of latent heat, respectively. Two or more samples were tested in each composition, and the measured values of the same composition were scattered in the range of 4 J/g. Similar magnitude of scattering was also seen in previous results [15,16].

In the upper figure, the peak temperature decreased monotonously with increasing Ni content; the change was small in Ti-rich side, while rapid decrease in Ni-rich side. Similar changes in the

Ms temperature have been reported [15,16]. In the lower figure, the present data almost agreed with the interpolation curves in previous studies [15,16]. The largest value observed in $Ti_{50}Ni_{50}$ was almost equal to or slightly larger than the solid line of Ref. [15].

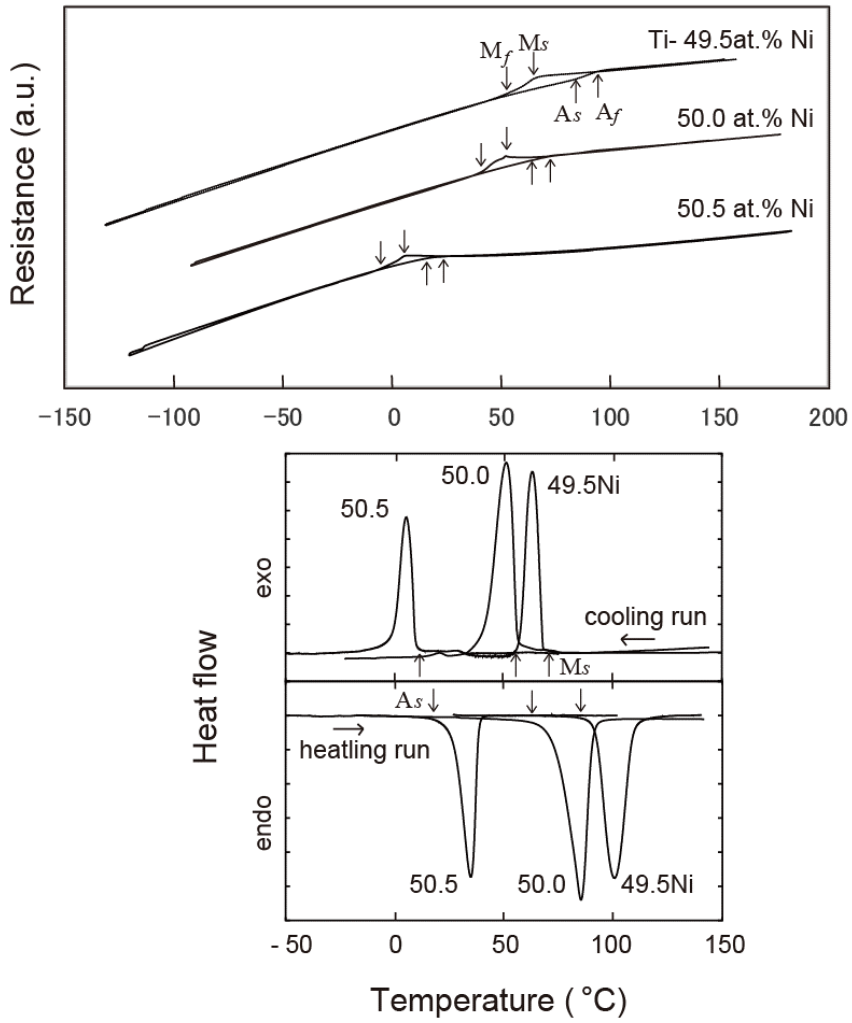

Fig.2 The electrical resistance and DSC curves of the solution treated Ti-49.5, 50.0, and 50.5 at.% Ni alloys. The Ms, Mf, As, Af temperatures are indicated by arrows.

The entropy of the transformation was examined. In constant pressure process, the entropy S [J/(gK)] is the sum of the infinitesimal change of entropy $\delta s = \delta Q/T$ and $\delta Q = \dot{Q}\delta t$, such that

$$S = \sum \frac{\delta Q}{T} = \int \frac{\dot{Q}(t)}{T} dt \ , \qquad (2)$$

where Q is the amount of latent heat per gram [J/g] and $\dot{Q}$ the rate of heat flow per gram [W/g]. The mean value theorem and Eq.1 gives the average approximately,

$$\langle S \rangle = \langle \int \frac{\dot{Q}}{T} dt \rangle \cong \frac{Q}{T_p} \ , \qquad (3)$$

where T_p is the peak temperature [K] defined above. This approximation may not cause significant amount of error as long as the hysteresis is narrow.

The entropy was calculated by Eq. 3 and plotted in Fig. 4. The figure agrees with the entropy 0.063 J/(gK) of $Ti_{49.5}Ni_{50.5}$ alloy reported in a previous study [36]. The figure shows that the entropy was different depending on the composition; the maximum presented at $Ti_{50}Ni_{50}$. The maximum was more marked than that of latent heat in Fig. 3.

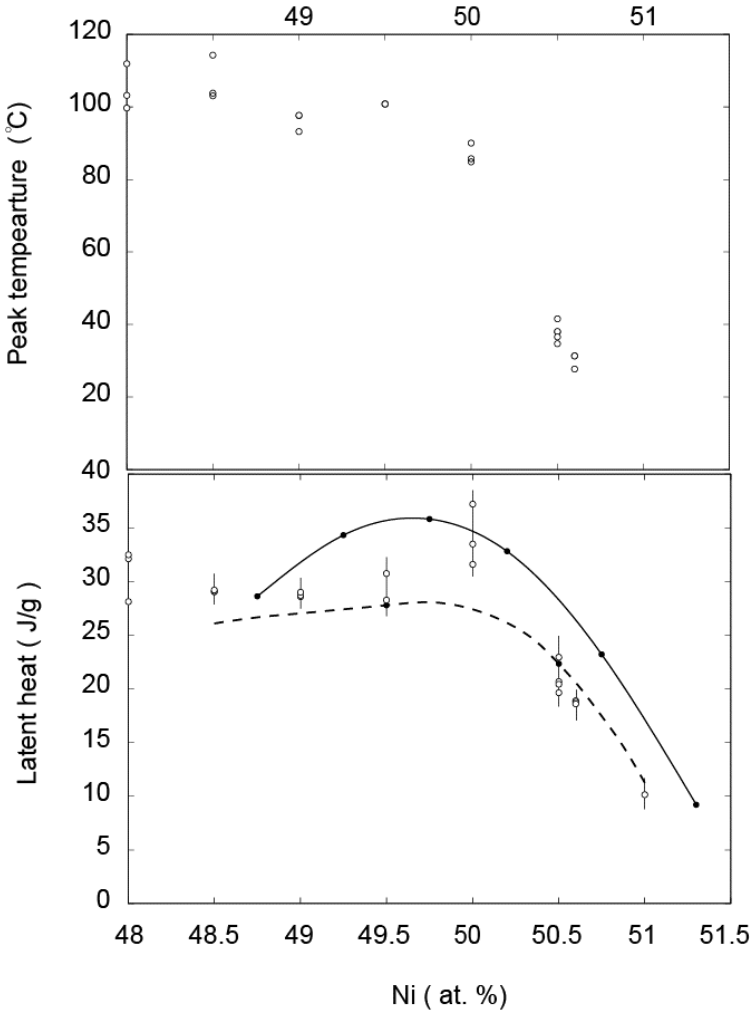

Fig. 3 Changes in the peak temperature and latent heat with Ni content in the solution treated NiTi alloys. The solid and dotted line in the lower figure is obtained from Ref. [15] and [16], respectively.

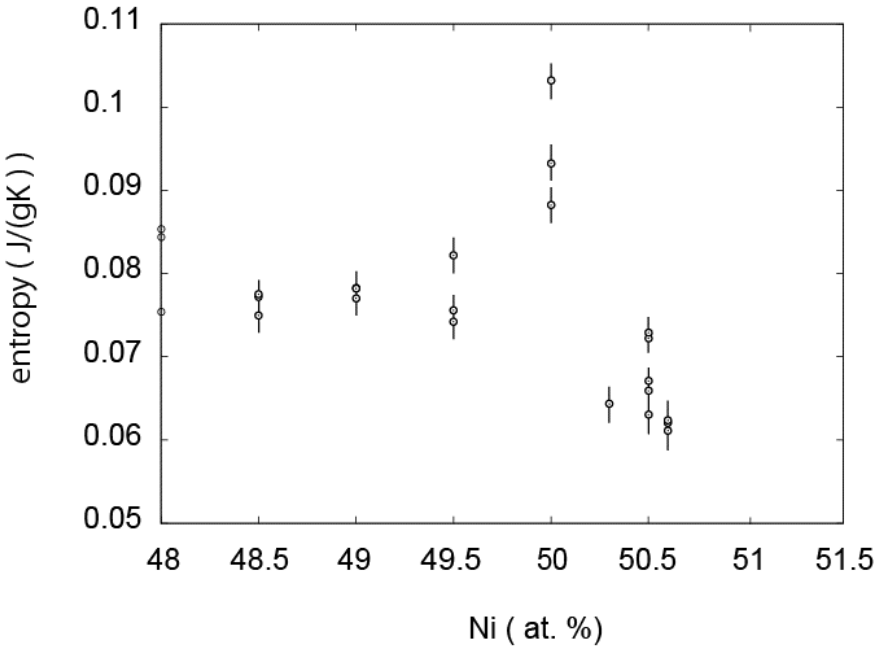

Fig. 4 The entropy of martensitic transformation calculated from Fig. 3 as a function of alloy composition.

The evidence for the reliability of measured was given in experiment. The transformation of the hot-rolled plate of $Ti_{50}Ni_{50}$ was measured simultaneously with the melting/solidifying reaction of a pure Indium by setting the NiTi sample on the sample stage of DSC and the Indium sample on the reference stage. Since the Indium was on the reference stage, the heat flow was measured in the reversed direction.

As shown in Fig. 5, the solidification heat emitted during cooling run was observed as an endothermic reaction (a downward peak) and the melting as an exothermic reaction (an upward one). In this figure, the latent heat of the forward (A to M) transformation and the reverse (M to A) one of NiTi was 36.2 J/g and −38.6 J/g, respectively, while the values of Indium 28.6 J/g and −28.3 J/g in accordance with the standard value of 28.45 J/g.

Considering the scattering of heat data, the data were collected from twenty-three samples prepared from the same plate of $Ti_{50}Ni_{50}$. Samples of thin round disks were made in order to be in thermal contact with the sample stage. The number distributions of the data in absolute values

are shown in Fig. 6(a), and the same data was plotted as a function of peak temperature in Fig. 6(b). It appears in both figures that the data points were distributed at random around the mean value. The average of latent heat was 34.8 J/g in the forward transformation and −37.8 J/g in the reverse transformation. The difference may be due to the hysteresis effect, which was the reverse transformation at higher temperatures than the forward transformation by letting the entropy of transformation be equal between the forward and reverse transformations. The slope of the linear approximation of Fig. 6(b) is 0.107 J/(gK). This value agrees with the maximum of entropy in Fig. 4.

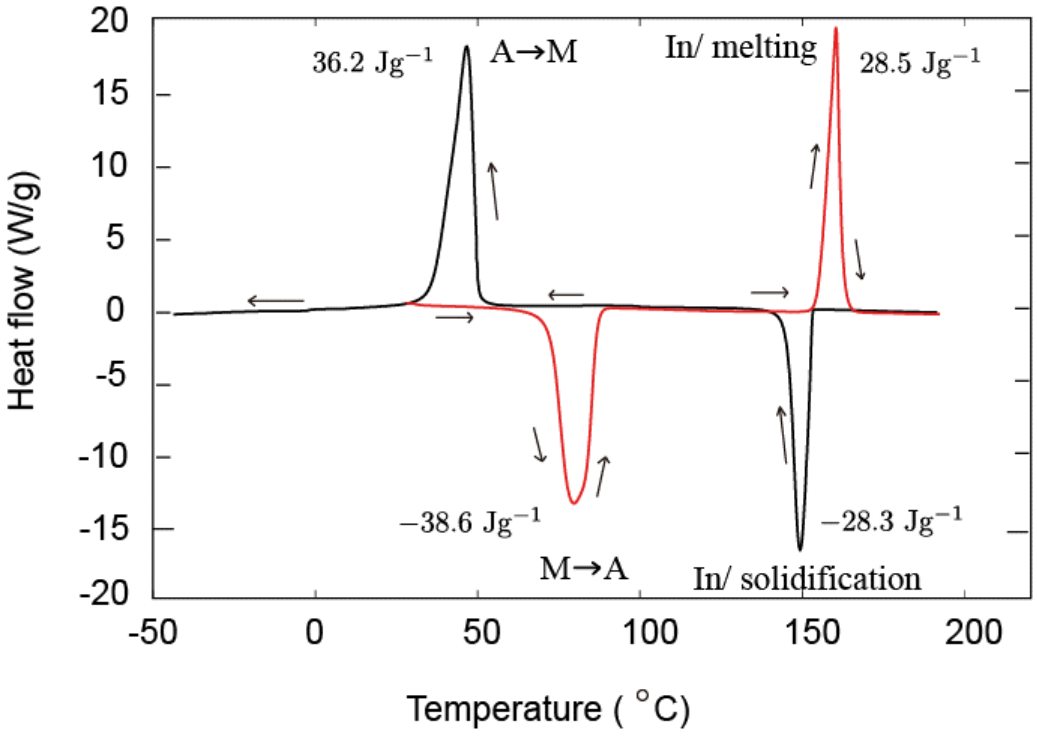

Fig. 5 The DSC profile of the simultaneous measurements of $Ti_{50}Ni_{50}$ and Indium. The heating and cooling run is drawn by red and black line, respectively. The heat flow of Indium was recorded in the reversed direction. The standard value of the latent heat of Indium is 28.45 J/g.

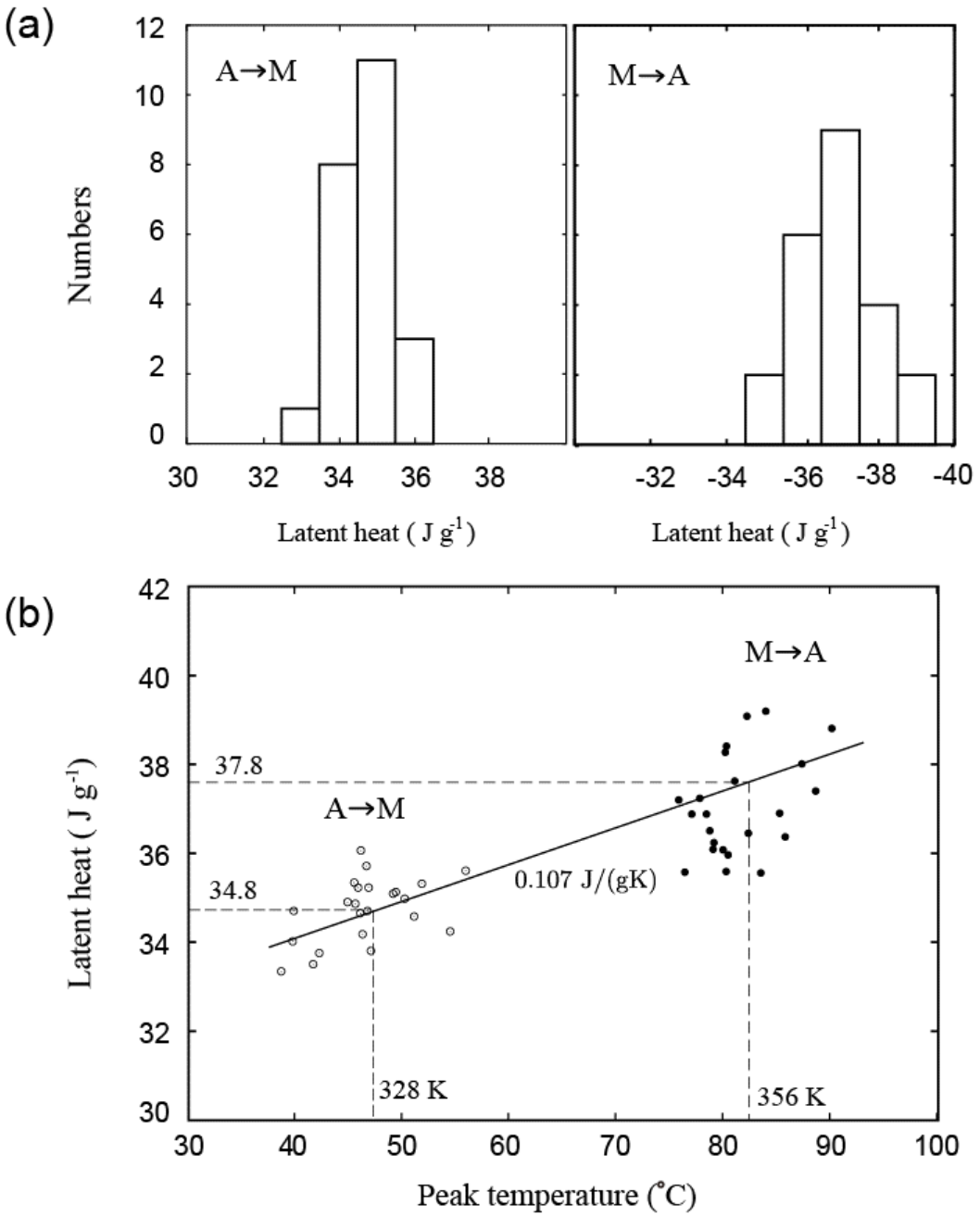

Fig. 6 The DSC data obtained in twenty-three samples of a solution treated $Ni_{50}Ti_{50}$ plate, (a) the number distribution of the latent heat in the forward transformation during cooling (left) and in the reverse transformation during heating (right), and (b) the relation between the absolute value of latent heat and the peak temperature of DSC curve.

Discussion

The magnitude is close to 51 J/g of VO_2 [37,38] and 60.3 J/g of Ti_3O_5 [39,40], which have been known as promising candidates for solid-state heat storage PCM. The density of $Ti_{50}Ni_{50}$ is 6.5 g/cm^3; the largest latent heat per unit volume of NiTi is 245 J/cm^3 in absorption and 226 J/cm^3 in emission, which are almost equal to those of PCM oxides, 233 J/cm^3 of VO_2 and 237 J/cm^3 of Ti_3O_5, as shown in Fig. 7.

In addition to the amount of heat, NiTi SMAs have some advantages in terms of formability, mechanical robustness, and the wide span of the transformation temperature controllable by alloying and/or materials processing.

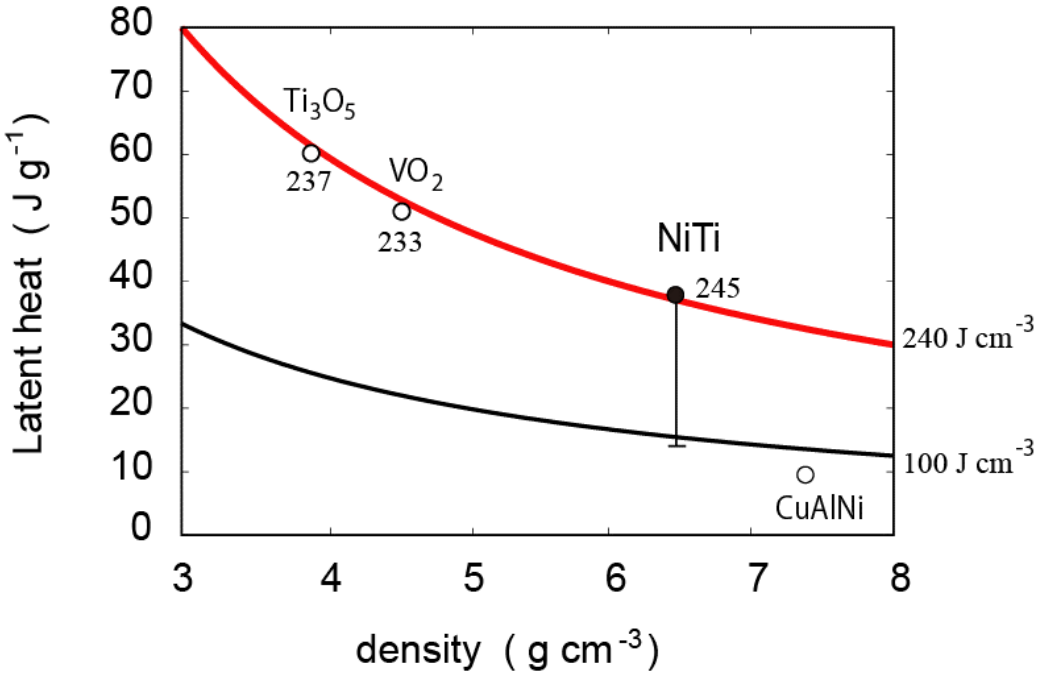

Fig. 7 The latent heat vs. density plot of SMAs, NiTi and CuAlNi, and ceramics, Ti_3O_5 and VO_2. The contour line is the amount of heat per unit volume. The present study determined the largest amount of latent heat in NiTi alloy.

Conclusions

It is demonstrated that the solution treated $Ti_{50}Ni_{50}$ alloy is a promising candidate for solid-state heat storage material. The alloy with the transformation hysteresis of 11 ℃ showed the latent

heat of −37.8 J/g in absorption and that of 34.8 J/g in emission. These values were larger than the largest value reported so far. Present study obtained the values in a commercial alloy with conventional purity. The values per unit volume of $Ti_{50}Ni_{50}$, −245 J/cm^3 and 226 J/cm^3, are comparable to those of VO_2 and Ti_3O_5, which are heat-storage ceramics under development.

Acknowledgment

This work was supported by MEXT/JSPS KAKENHI Grant number 19K0498109.

Compliance with Ethical Standards

The author declares that he has no conflicts of interest directly relevant to the content of this article.

REFERENCES

[1]Aprea C, Greco A, Maiorino A, Masselli C (2020) The employment of caloric-effect materials for solid-state heat pumping. Int J Refrigeration, 109: 1-11. https://doi.org/10.1016/j.ijrefrig.2019.09.011

[2]Bonnot E, Romero R, Manosa L, Vives E, Planes A (2008) Elastocaloric Effect Associated with the Martensitic Transition in Shape-Memory Alloys. Phys Rev Lett 100.125901. https://doi.org/10.1103/PhysRevLett.100.125901

[3]Wendler F, Ossmer H, Chluba C, Quandt E (2017) Mesoscale simulation of elastocaloric cooling in SMA films. Acta Mater 136:105-117. https://doi.org/10.1016/j.actamat.2017.06.044

[4]Manõsa L, Jarque-Farnos S, Vives E, Planes A (2013) Large temperature span and giant refrigerant capacity in elastocaloric Cu-Zn-Al shape memory alloys. Appl Phys Lett 103: 211904. https://doi.org/10.1063/1.4832339

[5]Tuśek J, Engelbrecht K, Mikkelsen LP, Pryds N (2015) Elastocaloric effect of Ni-Ti wire for application in a cooling device. J Appl Phys 117:124901. https://doi.org/10.1063/1.4913878

[6]Abhat A (1983) Low temperature latent heat thermal energy storage: heat storage materials. Solar Energy 30:313-332. https://doi.org/10.1016/0038-092X(83)90186-X

[7]Zare M, Ketabchi M (2017) Effect of chromium element on transformation, mechanical and corrosion behavior of thermomechanically induced Cu-Al-Ni shape memory alloys. J. Therm. Analysis Calorimetry 127: 2113–2123 https://doi.org/10.1007/s10973-016-5839-2

[8]Balo SN, Sel N (2012) Effect of thermal aging on transformation temperatures and some physical parameters of Cu-13.5wt.%Al-4at.%Ni shape memory alloy. Thermochimica Acta 536: 1–5. https://doi.org/10.1016/j.tca.2012.02.007

[9]Yang CH, Lin HC, Lina KM, Tsai HK (2008) Effect of thermo-mechanical treatment on a Fe-30Mn-6Si shape memory alloy. Mater Sci Eng A 497:445–450. https://doi.org/10.1016/j.msea.2008.07.057

[10]Czeppe T, Koval YN, Monastyrsky GE (1997) The microstructure and martensitic transformation in Ni-Al alloys with Yttrium addition. J Phys. IV France 7, C5: 173. https://doi.org/10.1051/jp4:1997527

[11]He Z, Zhou J (2003) Calorimetric investigation of martensitic transformation behavior in NiAlMnFe high-temperature shape memory alloy. J Mater Sci Lett 22: 375–376.

[12]Jiang C, Muhammad Y, Deng L, Wu W, Xu H (2004) Composition dependence on the martensitic structures of the Mn-rich NiMnGa alloys. Acta Mater 52:2779–2785. https://doi.org/10.1016/j.actamat.2004.02.024

[13]Wang Y, Huang C, Gao J, Yang S, Ding X, Song X, Ren X (2012) Evidence for ferromagnetic strain glass in Ni-Ti. Appl Phys Lett 101: 101913. https://doi.org/10.1063/1.4751250

[14]Liu J, Xia M, Huang Y, Zheng H, Li J (2006) Effect of annealing on the microstructure and martensitic transformation of magnetic shape memory alloys CoNiGa. J. Alloys Compounds 417 : 96-99. https://doi.org/10.1016/j.jallcom.2005.09.026

[15]Otubo J, Rigo O, Coelho A, Neto C, Mei P (2008) The influence of carbon and oxygen content on the martensitic transformation temperatures and enthalpies of NiTi shape memory alloys. Mater Sci Eng A 481-482: 639-642. https://doi.org/10.1016/j.msea.2007.02.137

[16]Frenzel J, George EP, Dlouhy A, Somsen Ch, Wagner M, Eggeler G (2010) Influence of Ni on martensitic phase transformations in NiTi shape memory alloys. Acta Mater 58: 3444-3458. https://doi.org/10.1016/j.actamat.2010.02.019

[17]Frenzel J, Wieczorek A, Opahle I, Maaβ B, Drautx R, Eggeler G (2015) On the effect of alloy composition on martensitic start temperatures and latent heats in Ni-Ti-based shape memory allos. Acta Mater 90: 213-231. https://doi.org/10.1016/j.actamat.2015.02.029

[18]Otsuka K, Sawamura T, Shimizu K (1971) Crystal structure and internal defects of equiatomic TiNi martensite. Physica Status Solidi 5: 457. https://doi.org/10.1002/pssa.2210050220

[19]Berman HA, West ED, Rozer AG (1967) Anomalous Heat Capacity of TiNi. J Appl Phys 38: 4473-4476. https://doi.org/10.1063/1.1709151

[20]Tang W, Sundman B, Sandstrom R, Qiu C (1999) New modelling of the B2 phase and its associated martensitic transformation in the Ti-Ni system. Acta Mater 47: 3457-3468. https://doi.org/10.1016/S1359-6454(99)00193-7

[21]Brailovski V, Terriault P, Prokoshkin S (2002) Influence of the post-deformation annealing heat treatment on the low-cycle fatigue of NiTi shape memory alloys. J Mater Eng Performance 11: 614-621. https://doi.org/10.1361/105994902770343593

[22]Hou H, Simsek E, Stassak D, Al Hasan N, Qian S, Otto R, Cui J, Takeuchi I (2017) Elastocaloric cooling of additive manufactured shape memory alloys with large latent heat. J. Phys. D: Appl. Phys. 50: 404001. https://doi.org/doi.org/10.1088/1361-6463/aa85bf

[23]Yasuda Y, Kato H, Sasaki K (2012) Clausius-Duhem inequality description of superelasticity in Ni-Ti polycrystal as dissipative process. Scripta Mater 66: 939–942. https://doi.org/10.1016/j.scriptamat.2012.02.036

[24]Wasilewski RJ, Butler SR, Hanlon JE, Worden D (1971) Homogeneity range and the martensitic transformation in TiNi. Metall Trans 2: 229-237.

[25]Murray JL, Phase Diagram of Binary Titanium Alloys (1987) The Ni-Ti System, ASM International 197-211.

[26]Tadayyon G, Mazinai M, Guo Y, Zeharjad SM, Tofail S, Biggs JP (2016) The effect of annealing on the mechanical properties and microstructural evolution of Ti-rich NiTi shape memory alloy. Mater Sci Eng A 662:546-577. https://doi.org/10.1016/j.msea.2016.03.004

[27]Khalil-Allafi J, Dloughy A, Eggeler G (2002) Ni_4Ti_3-precipitation during aging of NiTi shape memory alloys and its influence on martensitic phase transformations. Acta Mater 50: 4255-4274. https://doi.org/10.1016/S1359-6454(02)00257-4

[28]Miyazaki S, Ohmi Y, Otsuka K, Suzuki Y(1982) Characteristics of deformation and transformation pseudoelasticity in Ti-Ni alloys. J de physique, 43 supple 12: C4-255. https://doi.org/10.1051/jphyscol:1982434

[29]Todoroki T, Tamura H (1987) Effect of heat treatment after cold working on the phase transformation in TiNi alloy. Trans Japan Inst Metals, 28: 83-94. https://doi.org/10.2320/matertrans1960.28.83

[30]Michutta J, Somsen Ch, Yawny A, Dlouhy A, Eggeler G (2006) Elementary martensitic

transformation processes in Ni-rich NiTi single crystals with Ni_4Ti_3 precipitates. Acta Mater 54: 3525-3542. https://doi.org/10.1016/j.actamat.2006.03.036

[31]Khalil-Allafi J, Eggeler G, Schmahl WW, Sheptyakov D (2006) Quantitative phase analysis in microstructures which display multiple step martensitic transformations in Ni-rich NiTi shape memory alloys. Mater Sci Eng A 438-440: 593-596. https://doi.org/10.1016/j.msea.2006.02.143

[32]Fan QC, Zhang YH, Wang YY, Sun MY, Meng YT, Huang SK, Wen YH (2017) Influence of transformation behavior and precipitates on the deformation behavior of Ni-rich NiTi alloys. Mater Sci Eng A 700: 269-280. https://doi.org/10.1016/j.msea.2017.05.107

[33]Kwarciak J, Morawiec H (1988) Some interpretation problem of thermal studies of the reversible martensitic transformation. J Mater Sci 23: 551-557. https://doi.org/10.1007/BF01174684

[34]Kato H, Sasaki K (2012) Avoiding error of determining the martensite finish temperature due to thermal inertia in differential scanning calorimetry: model and experiment of Ni-Ti and Cu-Al-Ni shape memory alloys. J Mater Sci. 47: 1399-1410.K https://doi.org/10.1007/s10853-011-5919-4

[35]Yamashita F, Wakoh M, Ishikawa K, Shibata H (2017) In situ observation of nonmetallic inclusion formation in NiTi alloys. Mater Transactions, 58: 1729-1734. https://doi.org/10.2320/matertrans.M2017156

[36]Kato H, Yasuda Y, Sasaki K (2011) Thermodynamic assessment of the stabilization effect in deformed shape memory alloy martensite. Acta Mater 59: 3955-3964. https://doi.org/10.1016/j.actamat.2011.03.021

[37]Berglund CN, Guggenheim HJ (1969) Electronic properties of VO_2 near the semiconductor -metal transition. Phys Rev 185: 1022. https://doi.org/10.1103/PhysRev.185.1034

[38]Kato K, Lee J, Fujita A, Shirai T, Kinemuchi Y (2018) Influence of strain on latent heat of VO_2 ceramics. J Alloys Compounds 751, 30: 241-246. https://doi.org/10.1016/j.jallcom.2018.04.094

[39]Tokoro H, Yoshikiyo M, Imoto K, Namai A, Nasu T, Nakagawa K, Ozaki N, Hakoe F, Tanaka K, Chiba K, Makiura R, Prassides K, Ohkoshi S (2015) External stimulation - controllable heat-storage ceramics. Nature Comm 6: 7037. https://doi.org/10.1038/ncomms8037

[40]Ohkoshi S, Tokoro H, Nagasawa K, Yoshikiyo M, Jia F, Namai A (2019) Low-pressure-responsive heat-storage ceramics for automobiles. Scientific reports 9:1303 https://doi.org/10.10.1038/s41598-019-49690-0

EOF